*J. Earth Syst. Sci.* (2020)129 64
https://doi.org/10.1007/s12040-019-1335-y




# New evidence for a thin crust and magmatic underplating beneath the Cambay rift basin, Western India through modelling of EIGEN-6C4 gravity data

Avinash Kumar Chouhan[1,2,*], Pallabee Choudhury[1] and Sanjit Kumar Pal[2]

[1]*Institute of Seismological Research, Gandhinagar 382 009, India.*
[2]*Department of Applied Geophysics, Indian Institute of Technology (Indian School of Mines), Dhanbad 826 004, India.*
**Corresponding author. e-mail: akchouhan31@gmail.com*

MS received 5 January 2019; revised 1 November 2019; accepted 15 November 2019

The Cambay rift basin (CRB) is an intracratonic rift in the western part of India. The basin assumes great importance in petroleum exploration owing to the presence of thick hydrocarbon bearing sedimentary rocks. Previous investigations using deep seismic soundings (DSS), gravity and heat flow data reveal that the CRB is characterised by a thin crust, high heat flow and high density lower crust. In this study, a detailed crustal structure of the basin is presented by performing a 2.5D density modelling of the EIGEN-6C4 gravity data. Present study attempt to find a plausible explanation for the variation in the Bouguer anomaly (BA) values from +20 to −50 mGal within the basin. It refined the crustal model that is constrained using results from radial average power spectrum (RAPS) analysis of gravity data along with previous seismological and geophysical studies, which reveals that the values of average sedimentary and Deccan Traps thickness are in the order of 4–5 and 1.5–3 km, respectively, along the rift. It also presents possible evidences for a high density underplated layer of thickness 7–15 km along the central part of the CRB. To study the deep-seated features, upward continuation of the BA is carried out at heights of 30, 40 and 50 km. The extension of underplating layer is noticed in the present crustal model and in the upward continued BA in the western part, while it merges with the Moho in eastern part of the CRB. The Moho depths, varying from 31 to 37 km, are found to be shallower inside the CRB than the surroundings. It is inferred that the high BA values in the basin are due to the combined effect of the high density underplated layer in the lower crust and a shallow Moho.

**Keywords.** Cambay rift basin; EIGEN-6C4 gravity data; underplated layer; 2.5D density modelling.

## 1. Introduction

Intracratonic rift basins are tectonic depressions in the Earth's surface, which are generally formed within the stable cratonic platform (Withjack *et al.* 2002; Thybo and Nielsen 2009). These intracratonic basins originate from lithospheric thinning and subsidence (White and McKenzie 1989) and assume great importance in the hydrocarbon-bearing provinces throughout the world. In the western margin of India, three intracratonic rift basins, namely, Kachchh, Cambay and Narmada, have been formed during the northward drifting of the Indian plate in early Jurassic, early Cretaceous and late Cretaceous, respectively (Biswas 1982, 1987). The Cambay graben is one of these three major marginal rift basins, which developed subsequently from north to south during India's

Published online: 06 February 2020

drift after the break-up of the Gondwanaland (Biswas 1982).

The Cambay basin is a rift basin forming the inland extension of the large offshore west coast basin and located on the west–northwest margin platform of the Indian craton (figure 1). The basin has been studied extensively towards petroleum exploration and for its crustal configuration. Previous geological and geophysical studies reveal that basin is characterised by a large sedimentary thickness and has favourable conditions for oil and gas prospecting (Biswas 1982; Kaila *et al.* 1990). It is already established as one of the most promising producing oil fields in India (DGH GOI 2017). The basin also has potential for hosting geothermal energy sources (Mohan *et al.* 2017). High heat flow values of 75–93 mW/m$^2$ are found in the northern Cambay basin (Gupta 1981). Curie depth (corresponding to an isotherm of ∼550°C) is estimated approximately at the depth of 22 km (Thiagarajan *et al.* 2001). Kaila *et al.* (1990) carried out DSS studies to delineate the crustal structure of the Cambay basin. Results of their studies indicate the presence of two different sedimentary layers, the average cumulative thickness to be 4–5 km along the DSS profile in the basin. Deccan Trap basalt form the basement to the sedimentary rocks, and the maximum depth to basement was found to be about 7.7 km in the Gandhinagar region. The studies of Kaila *et al.* (1990) and Dixit *et al.* (2010) found the Moho depth to vary in the range 31–33 km in the north Cambay basin and 31–37 km in the south Cambay basin. Chopra *et al.* (2014) estimated the Moho depth to be 36.5 km in the Gandhinagar region and 35 km in Radhanpur region, based on the analysis of teleseismic receiver functions. Further, Rao *et al.* (2015) calculated the average Moho depth to be 32.7 ± 2.59 km with $V_P/V_S$ value of 1.67 ± 0.27 in the Cambay basin, based on H-k stacking analysis of receiver functions.

Results of previous gravity studies conducted in the CRB reveal presence of the higher regional Bouguer anomaly (BA) values within the basin than outside (Avasthi *et al.* 1971; Tewari *et al.* 1991, 2009). The high gravity values have been attributed to uplift of the Moho and shallow depth

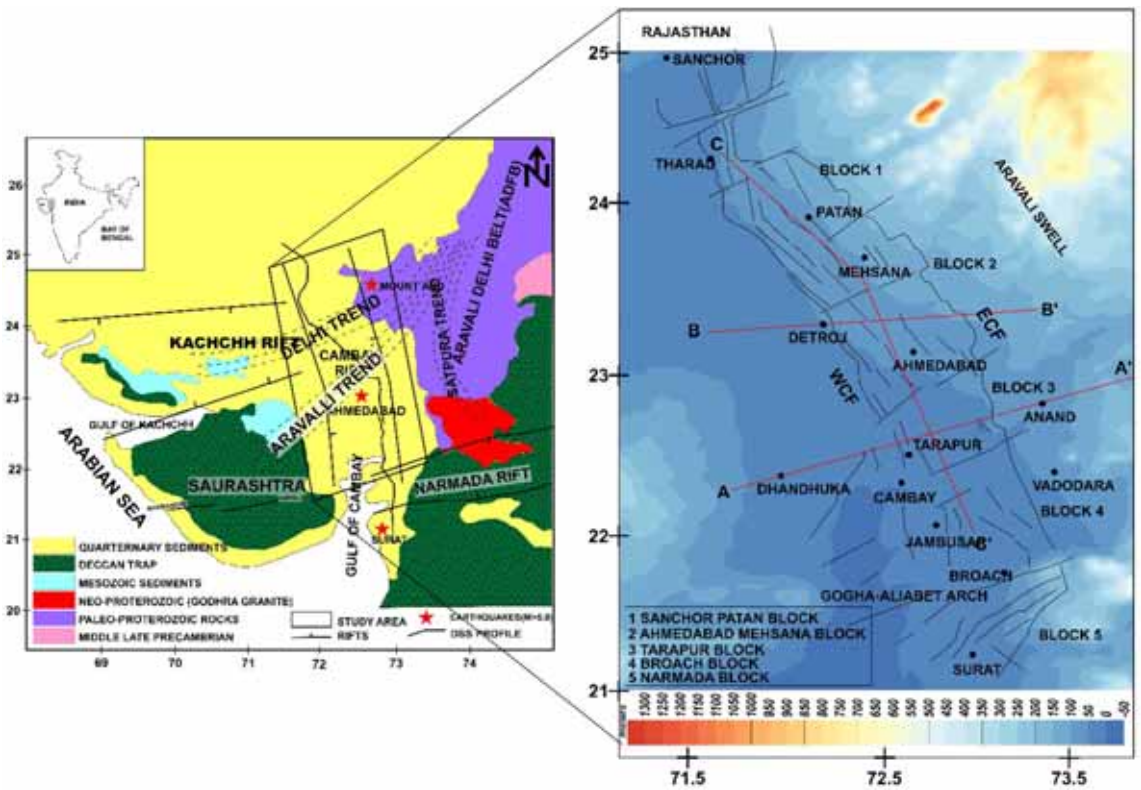


Figure 1. Generalised geological map of the Cambay rift basin and adjacent area (after Biswas 1987 and Krishnamurthy *et al.* 2000). Insight: Detailed tectonic map of the study area (after Dhar and Bhattacharya 1993 and Mishra and Patel 2011) overlain on the elevation. Red lines AA′, BB′ and CC′ are the profiles used for gravity modelling. Map also shows the DSS profile (after Kaila *et al.* 1990 and Dixit *et al.* 2010) by black thick line and epicentre of the earthquakes ($M$>5.0) in the CRB (after Chandra 1977 and Gupta *et al.* 1972). Sanchor–Patan, Ahmedabad–Mehsana, Tarapur, Broach and Narmada blocks are represented as Block 1, 2, 3, 4 and 5, respectively.

of the mantle, larger thickness of the volcanics within the basin (Kailasam and Quereshy 1964), and crustal thinning with high density lower crust (Tewari *et al.* 1991; Radha Krishna *et al.* 2002). Results of Tewari *et al.* (1991) also reveal presence of magmatic underplating within the basin.

Global gravity field models are used in regions with difficult accessibility and poor *in-situ* data coverage. EIGEN-6C4 (European Improved Gravity model of the Earth by New techniques-6C4) is a static global combined gravity field of the Earth, based on satellite gravity observations by GRACE and GOCE satellites, EGM 2008 gravity model and DTU10, which also include the latest ArcGP solutions (Tapley *et al.* 2004; Forsberg and Skourup 2005; Anderson *et al.* 2010; Pavlis *et al.* 2013; Förste *et al.* 2014). The global gravity field model data have used for different geological and hydrocarbon exploration over parts of India (Pal and Majumdar 2015; Vaish and Pal 2015; Pal *et al.* 2016; Narayan *et al.* 2017). Pal and Majumdar (2015) used GOCE, EIGEN6-C2 and *in-situ* gravity data for geological appraisal over the Singhbhum–Orissa Craton, India. Structural mapping over the 85°E ridge and surroundings have been effectively carried out using EIGEN6C4 and other Global Combined Gravity Field Model data (Narayan *et al.* 2017).

Gravity modelling is very useful for the delineation of crustal structures, if the density configuration is well constrained. The results of stochastically generated forward gravity anomalies can be compared with the observed gravity anomalies to find density models that match with the observed data. In the present study, the high resolution EIGEN-6C4 gravity data have been used to perform 2.5D gravity modelling for delineation of detailed crustal structure of the Cambay basin. To constrain the density configuration, we used the geological, seismological and other geophysical inputs from previous studies and estimated the sedimentary thickness along the Cambay basin. Present study attempt to explore the spatial extent of the magmatic underplating layer and to elucidate the reason of the crustal thinning within the basin. Although the presence of underplated layer with crustal thinning and Moho upwarping in the CRB has already been established by previous studies (Kaila *et al.* 1990; Tewari *et al.* 1991; Dixit *et al.* 2010), the extent/limit of the magmatic underplating was poorly understood, which is revealed in the present study. A detailed subsurface crustal structure of the CRB has been elucidated with the new data sets, considering input from recent seismological and geophysical studies. Results of our study also illuminates on the probable causes of the high Bouguer anomalies within the CRB.

## 2. Geology and tectonics of the CRB

The Cambay basin is roughly limited by latitudes 21°–25°N and longitudes 71°30′–73°30′E (figure 1). It covers an approximate area of 53,500 km$^2$ (DGH GOI 2017). The Cambay basin is separated from the Rajasthan basin by a basement swell to the north of Sanchor (figure 1). It then extends about 450 km along an almost north–south direction to the Gulf area and widens up to 80 km. Further, it merges in the south with the Surat depression of the Bombay offshore basin across the Gogha–Aliabelt basement arch (figure 1) (Dhar and Bhattacharya 1993; Merh 1995; Mishra and Patel 2011). The basin narrows towards the north direction in the Sanchor region, while it widens in the southern part (Kundu *et al.* 1993). From north to south, the Cambay basin extends approximately in NW–SE direction up to 21°45′N latitude and thereafter it changes its direction in NNW–SSE towards the Gulf of Cambay. It is surrounded by Saurashtra uplift in the west, Aravalli–Delhi older Proterozoic rocks belt in the northeast, the ENE–WSW trending Narmada rift in its south, ENE–WSW trending Kachchh rift in the northwest and Deccan Traps of late Cretaceous age in the southeast (Biswas 1982, 1987). The Aravalli trend (NE–SW) continues further southwest underneath the CRB and Saurashtra peninsula, whereas the Delhi trend (NE–SW) runs approximately in the direction of east–west under the Kachchh rift (Biswas 1982).

The sedimentary geology of the CRB is well known from Tertiary to recent deposits because of the different large scale oil exploration programmes of Oil and Natural Gas Corporation (ONGC), India. The basin is filled with Quaternary and Tertiary sediments mainly consisting of sandstone, siltstone, claystone and shale (Biswas 1982, 1987; Merh 1995). These sediments were deposited on the floor of the volcanic Deccan Traps (basalts), and it is suspected that Mesozoic sediments are also present below the volcanics (Avasthi *et al.* 1971; Biswas 1982, 1987; Kaila *et al.* 1990; Tewari *et al.* 1991, 2009; Dixit *et al.* 2010; Nabhakumar *et al.* 2012). The Cambay basin is bound by the

well demarcated basin marginal faults, East and West Cambay faults (figure 1). A number of NE–SW trending faults divide the Cambay rift into five tectonic blocks, from north to south. These are Sanchor–Tharad block, Mehsana–Ahmedabad block, Cambay–Tarapur block, Jambusar–Broach block and Narmada block (figure 1) (Dhar and Bhattacharya 1993; DGH, GOI 2017). The tectonics of the CRB is affected by three major Precambrian trends: Dharwar (NNW–SSE), Aravalli–Delhi (NE–SW) and Satpura (ENE–WSW) trends (Kundu *et al.* 1993). Subsurface data indicates presence of pre-existing step faults parallel to the Eastern Cambay marginal fault. Most of these faults are NNW–SSE trending, except some that are trending ENE–WSW (Mishra and Patel 2011) (figure 1).

## 3. Data and methodology

We used EIGEN-6C4 gravity data generated from the International Centre for Global Earth Models (ICGEM) at a grid interval of 0.1° (Förste *et al.* 2014). The data is available up to the maximum degree and order of 2190 (Förste *et al.* 2014). Topographic corrections (Bouguer plate and terrain correction) were done before preparing the BA map. The Bouguer plate correction accounts for the all topographic masses above the sea level and it is calculated by applying the Bouguer plate correction $2\pi\rho Gh = 0.0419h$, where $G$ is universal gravity constant equal to $6.67\times10^{-11}$ m$^3$ kg$^1$ sec$^{-1}$, $\rho$ is constant density of Bouguer slab, $h$ is topographical height in m. The BA is calculated by using digital elevation model ETOPO1 for topographical heights and a density of 2.67 gm/cc for the Bouguer slab. The BA map is prepared by using minimum curvature gridding method with a grid size of 0.01° and shown in figure 2(a).

The main advantage of using satellite gravity data is that it gives spatially uniform coverage, comprising all possible medium to long wavelengths which is free from ruggedness and remoteness of the terrain, while terrestrial survey is suitable for short wavelength data analysis which yields gravity values at points (Bomfim *et al.* 2013). Previous studies argue for the suitability of satellite based combined Global Earth Models and also indicate very good correlation with the terrestrial gravity data (Bomfim *et al.* 2013; Pal and Majumdar 2015; Vaish and Pal 2015; Pal *et al.* 2016; Narayan *et al.* 2017). The satellite gravity data would allow correct calibration of terrestrial gravity data by adding enormous value to the latter that enhances the spatial resolution. To compare the resolution of the satellite based gravity data with the available terrestrial data (Tewari *et al.* 2009), the BA values at 11 points have been noted where major anomalies are observed (figure 2b). The values at these 11 points and the difference in them are shown in table 1. Moreover, the available land based BA map (after Tewari *et al.* 2009) is shown in figure 2(b), along with figure 2(a), for a qualitative comparison. It is observed that maximum absolute difference between the amplitude of EIGEN-6C4 and terrestrial Bouguer anomaly is about −6.9 mGal with correlation value of 0.99 (table 1). The gravity highs H1, H4, H5 and H6 in the EIGEN-6C4 data have the similar amplitude and pattern with the gravity highs 3, 7, 5 and 6 in the terrestrial data, respectively. Likewise, the gravity lows L1, L2 in the EIGEN-6C4 data have the similar amplitude and pattern with gravity lows at 4, 8 in the terrestrial gravity data, respectively (figure 2, table 1). The comparison between the Bouguer anomalies of the two data sets show considerable consistency for both the long and short wavelength anomalies over the CRB (figure 2).

Upward continuation (UC) at different height of the BA is done to study the deep seated features. UC accentuates the long wavelength anomalies (correspond to deeper features) and attenuates the shorter wavelength anomalies (correspond to shallow features) and used as the optimum filter to extract regional anomaly from gravity data (Rao and Murthy 1978; Blakely 1995). It is done by transforming the gravity data measured on one surface to another surface at different heights (Blakely 1995; Jacobsen 1987; Zeng *et al.* 2007). According to Jacobsen (1987), the regional field calculated by upward continuation of gravity anomaly at height $z$ is associated to sources seated at half the height of UC, that is, $z/2$. Following Jacobsen (1987), the Bouguer anomaly is upward continued to the heights of 30, 40, and 50 km to study the deep seated features at depths 15, 20 and 25 km, respectively.

Gravity anomaly constitutes different longer wavelengths (smaller wavenumbers) and shorter wavelengths (higher wavenumbers), correspond to deeper and shallow features, respectively, and it originates due to different density bodies within the Earth (Lowrie 2007). To get the estimates of average depth to the source, the radial average

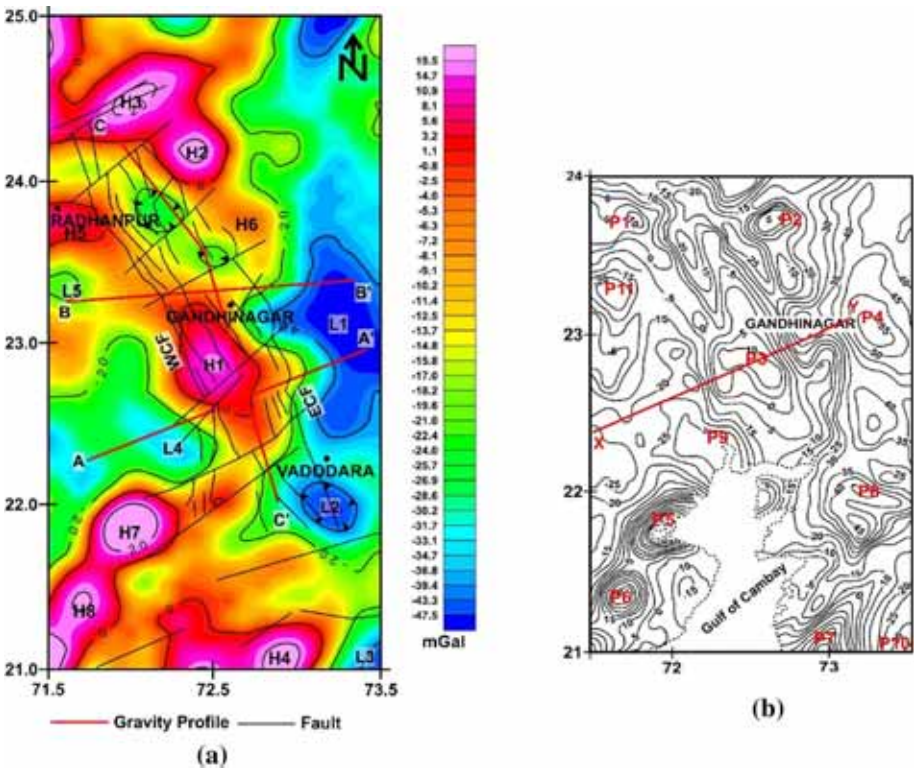


Figure 2. **(a)** EIGEN-6C4 Bouguer anomaly of the Cambay rift basin. AA′, BB′ and CC′ are the profiles used for gravity modelling. Eight gravity highs H1–H8 and five gravity lows (L1–L5) have been identified. Basin marginal faults (ECF: Eastern Cambay Fault and WCF: Western Cambay Fault) are also shown. Black lines represent the faults. Red lines AA′, BB′ and CC′ are the profiles used for gravity modelling. **(b)** Terrestrial Bouguer anomaly map of contour interval of 5 mGal of the Cambay rift (after Tewari *et al.* 2009). Anomaly values given in the contours are in mGal. Total 11 points (P1–P11, written in red) corresponding to different BA highs and lows observed in the EIGEN-6C4 Bouguer anomaly are opted for data comparison. XY is the profile used for comparative gravity modelling of EIGEN-6C4 Bouguer anomaly with the terrestrial.

Table 1. *Amplitude difference between EIGEN-6C4 and terrestrial Bouguer anomaly values at different points. The correlation factor is 0.99. Locations of the comparison points are shown in figure 2.*

| Location of comparison points | | EIGEN-6C4 Bouguer anomaly | | Terrestrial Bouguer anomaly (after Tewari *et al.* 2009) | | |
|---|---|---|---|---|---|---|
| Lon. (°E) | Lat. (°N) | High/low | Amplitude (mGal) | Point no. | Amplitude (mGal) | Difference (mGal) |
| 71.6 | 23.75 | H5 | 6.6 | P1 | 5 | 1.6 |
| 72.7 | 23.75 | H6 | −5.1 | P2 | −5 | −0.1 |
| 72.5 | 22.9 | H1 | 16.4 | P3 | 15 | 1.4 |
| 73.2 | 23.2 | L1 | −54.6 | P4 | −55 | 0.4 |
| 72 | 21.9 | H7 | 40.3 | P5 | 40 | 0.3 |
| 71.7 | 21.4 | H8 | 23.1 | P6 | 30 | −6.9 |
| 72.9 | 21.1 | H4 | 27.4 | P7 | 30 | −2.6 |
| 73.2 | 22 | L2 | −47.6 | P8 | −45 | −2.6 |
| 72.25 | 22.35 | L4 | −35.3 | P9 | −30 | −5.3 |
| 73.5 | 21 | L3 | −37.1 | P10 | −35 | −2.1 |
| 71.65 | 23.25 | L5 | −18.4 | P11 | −20 | 1.6 |

power spectrum analysis has been done by employing Fast Fourier transformation of the Bouguer anomaly, using GEOSOFT (Oasis Montaj MAGMAP manual; Spector and Grant 1970). Initially, the power spectrum was established for magnetic anomaly and later it was generalised for

the gravity anomaly (Maus and Dimri 1996). A simple relation is established by Spector and Grant (1970) between power spectrum and source depth that is expressed as:

$$P(k) = A * \exp(-2|k|h). \quad (1)$$

With logarithm in both sides the above equation yields

$$\ln(P) = -2|k|h + A, \quad (2)$$

where $P(k)$ is power spectrum, $k$ is wavenumber, $A$ is a constant and $h$ is the depth to the top of anomaly. Spector and Grant (1970) have considered that anomaly resulted due to magnetic source are the combined result of a large number of blocks and probability distribution of all the blocks is equal to the parameter of one block. The gridded anomaly data is used by Spector and Grant (1970) for the calculation of two-dimensional power spectrum and then they used annular averages to find the depths of the causative anomaly due to the uncorrelated distribution of the ensemble of prismatic bodies. The natural logarithm of the amplitude is then plotted against the wavenumber. The mean depth of the source is calculated by the slopes of the best fitting straight lines via a least-squares regression and multiplying by $1/4\pi$ (Mishra 2011; Spector and Grant 1970). Spector and Grant (1970) suggested that more than one straight line can be fitted. The calculated depths give the estimation for the average depth to the top of the source bodies (Maus and Dimri 1996).

2.5D forward gravity modelling is then carried out using commercial software package GMSYS (Oasis Montaj GMSYS manual) to map the detailed crustal structure of the basin. The modelling involves calculation of the gravity response due to multiple polygonal shaped bodies of finite strike length based on the formulation of Talwani *et al.* (1959). Gravity models provide valuable insight into the geological understanding; however, non-uniqueness is the inherent problem in derivation of geological section from the modelling of gravity data (Dobrin and Savit 1988; Lowrie 2007). Keeping this view of non-uniqueness and dependence of gravity on density and depth, constraints from power spectrum analysis of BA, DSS (Kaila *et al.* 1990; Dixit *et al.* 2010), receiver function analysis (Chopra *et al.* 2014), and well data (Pandey 2012) have been used for the modelling. We performed 2.5D gravity modelling along the three profiles AA′, BB′ and CC′. Profiles AA′ and BB′ are taken across the basin and CC′ is taken along the basin, as shown in figures 1 and 2. These three profiles are chosen in such a way that it can be possible to validate the gravity values at the particular point where they intersect. It will also enable us to see the gravity anomalies at the boundaries as well as along the basin. The depth and velocity information used in the modelling are derived from the DSS and receiver function results of the study area (figure 3). Well data is used to constrain the shallow part (sedimentary and trap layer) of the rift. Densities for modelling have been estimated by converting P wave velocities obtained from the DSS results. Towards doing so, we used the conversion function following Ludwig *et al.* (1970), Barton (1986), Christensen and Mooney (1995) and Brocher (2005). The densities of the layer thus estimated and corresponding stratigraphic units used for modelling are shown in table 2. Kaila *et al.* (1990), Tewari *et al.* (1995), Dixit *et al.* (2010) and Pandey (2012) indicated presence of very thin layer of Mesozoic, which has a very small gravity response. Hence, the Mesozoic layer is not considered while doing the modelling.

## 4. Results and discussion

The BA map prepared for Cambay rift is shown in figure 2(a). The BA values range from +20 to −50 mGal. Eight gravity highs (H1–H8) and five gravity lows (L1-L5) have been identified (figure 2a). Some circular (H1, H2 and H4) and elliptical (H3) shaped high gravity anomalies are found which are indicative of three dimensional source (Rao and Murthy 1978). Presence of a high density underplated layer in the lower crust (Tewari *et al.* 1991) is attributed to be the reason for high gravity H1. The gravity highs H2 and H3 reflect the Delhi–Aravalli trend, which passes through the Cambay basin. The reason for high Bouguer value H4 may be the presence of shallow basement in the area (Dixit *et al.* 2010) or presence of mafic body of density 2.9 gm/cc in the upper crust (Bhattacharji *et al.* 2004). Gravity lows L1 and L2 are also observed, the reasons are discussed at a later part. The boundary between gravity anomalies H1 and L4 distinctly image the boundary of the West Cambay Fault (WCF). The boundary of the East Cambay Fault (ECF) is clearly marked between gravity anomalies H1 and L1, only in the north of the profile BB′. In the south of BB′, L2 exists, reflecting presence of a deep-seated basement

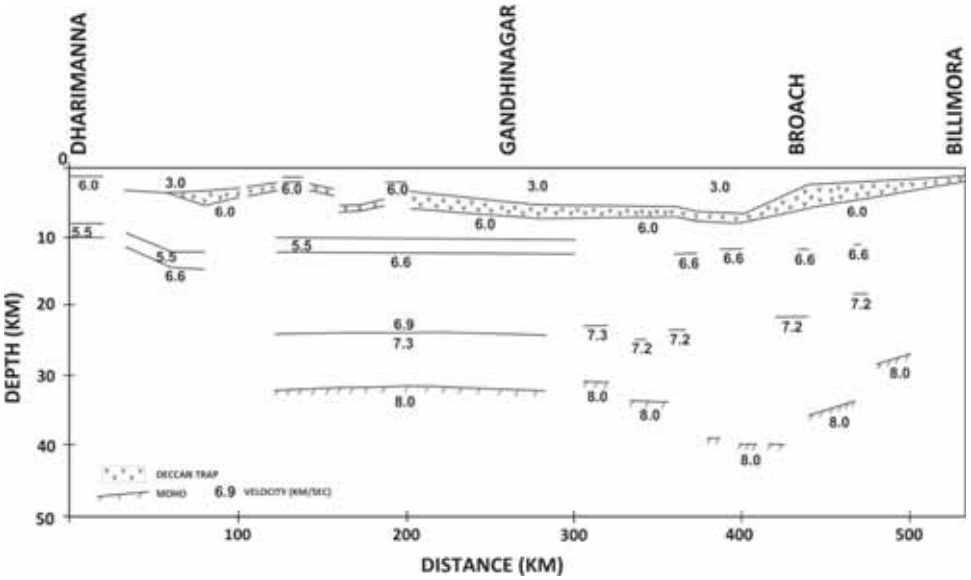


Figure 3. Crustal velocity depth model along the DSS profile in the Cambay rift basin (after Kaila *et al.* 1990 and Dixit *et al.* 2010).

Table 2. *Densities and corresponding stratigraphic units used for the modelling.*

| Density (gm/cc) | Stratigraphic unit |
|---|---|
| 2.2 | Quaternary and Tertiary |
| 2.4 | sediments |
| 2.8 | Deccan traps |
| 2.67 | Pre-Cambrian basement |
| 2.85 | Lower crust |
| 3.15 | Magmatic underplated layer |
| 3.3 | Upper mantle |

(depth ∼9.5 km) in the Broach area (Singh and Meissner 1995; Dixit *et al.* 2010).

Source depth estimation using power spectrum analysis is done which is used as a first-hand information for modelling constraints. The radial average power spectrum of BA of the Cambay basin is plotted and shown in figure 4. From the power spectrum, two best fitted regression lines are observed using least square method and the regression lines are defined by equations $y = -262 * x + 7.22$ and $y = -65 * x + 0.325$, where $x$ is wavenumber and $y$ is ln (power). The two regression lines give the depths to the top of interfaces at 5.2 and 21 km. The 5.2 km depth segment corresponds to high wavenumber and it can be interpreted as the density contrast at the basement. The 21 km depth segment corresponds to low wavenumber, which is related to the deeper part of the crust. It is observed that the spectral depth to

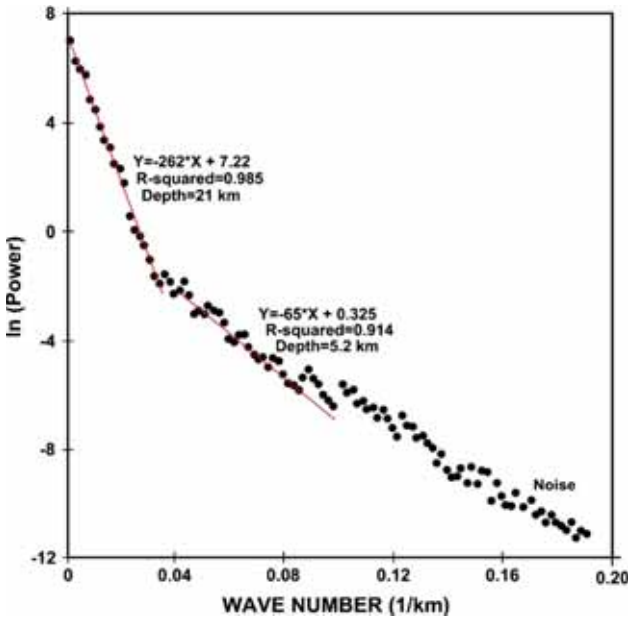


Figure 4. Power spectrum of the BA values of the Cambay rift basin showing logarithm of BA spectrum as a function of wavenumber, giving the fitted linear segments related to sources at two different depths, 5.2 and 21 km.

the basement (5.2 km) and the boundary between middle and lower crust (21 km) are almost the same as that inferred from DSS and seismological data (Kaila *et al.* 1990; Dixit *et al.* 2010; Chopra *et al.* 2014). It is worth mentioning here that according to Studinger and Miller (1999), depth estimation using the power spectrum analysis of BA depends on two aspects. First, the study area should contain uniform crustal architecture and

second, it should be large enough to resolve long wavelengths Bouguer anomalies. In the present study, the area opted for power spectrum analysis is not large enough to resolve the longer wavelengths corresponding to deeper feature like the crust-mantle boundary.

The density model of the 200 km long profile AA′ is shown in figure 5(a). It is observed that the Bouguer values are high in the central part of the basin and decrease towards both the flanks. We adopted the crustal structure configuration from DSS result (figure 3) for the gravity modelling along AA′ section. Shallow part of the rift is constrained by well drilled in Dhandhuka and Anand which encountered Pre-Cambrian basement at depth 1.3 and 1.6 km, respectively (Rao and Tewari 2005; Pandey 2012). The lithology of the wells are shown in figure 5(a). Based on density model, total thickness of sedimentary rocks is found to be 5 km in the central part, which tapers towards both the marginal faults of the basin (figure 5a). The thickness of the Deccan Traps is maximum (2–3 km) in the central part and it decreases towards the flanks of the rift. Thickness of upper crust is about 6 km along the profile. The model elucidates that high density (3.15 gm/cc) underplating layer is present in lower crust. Thickness of the underplated layer is maximum in central part of the rift and decreases towards the WCF while it merges with Moho in eastern part of

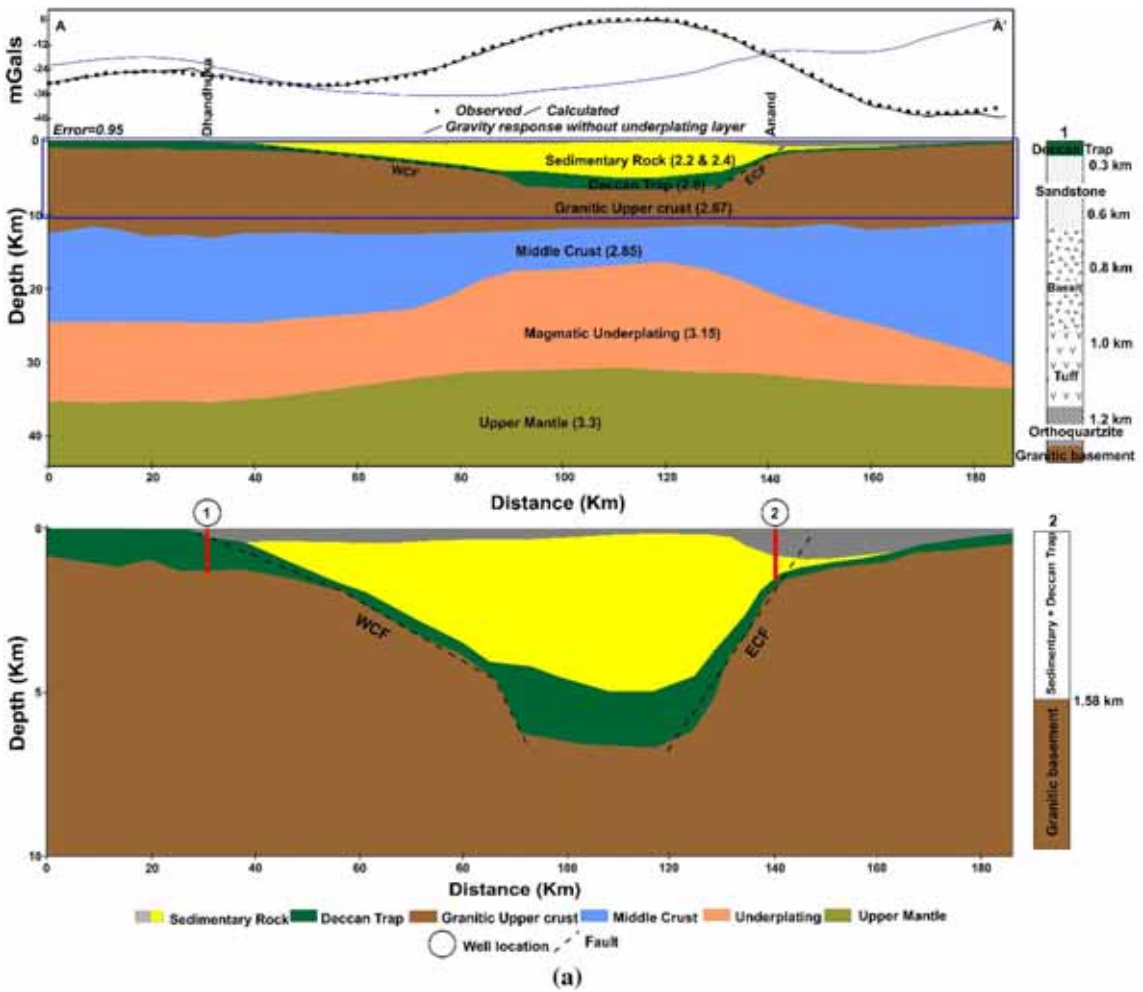


Figure 5. Density model along the profiles **(a)** AA′, **(b)** BB′, and **(c)** CC′. Zoomed part of blue box covering 10 km depth section are shown below in each figures (a) and (b). ECF and WCF correspond to Eastern Cambay and Western Cambay faults (locations shown as black dashed lines). Numbers show densities in gm/cc. Well locations are shown in the model by circles and lithology is presented along with the model. Wells encountered Pre-Cambrian basement are shown by vertical red lines in the model. 1: Dhandhuka well, 2: Anand well and 3: Detroj well (Rao and Tewari 2005; Pandey 2012). **(d)** EIGEN-6C4 gravity data and modelled gravity response computed using density model of Tewari *et al.* (1991) along profile XY. The observed values are represented by black dots and the computed response is shown by black line.

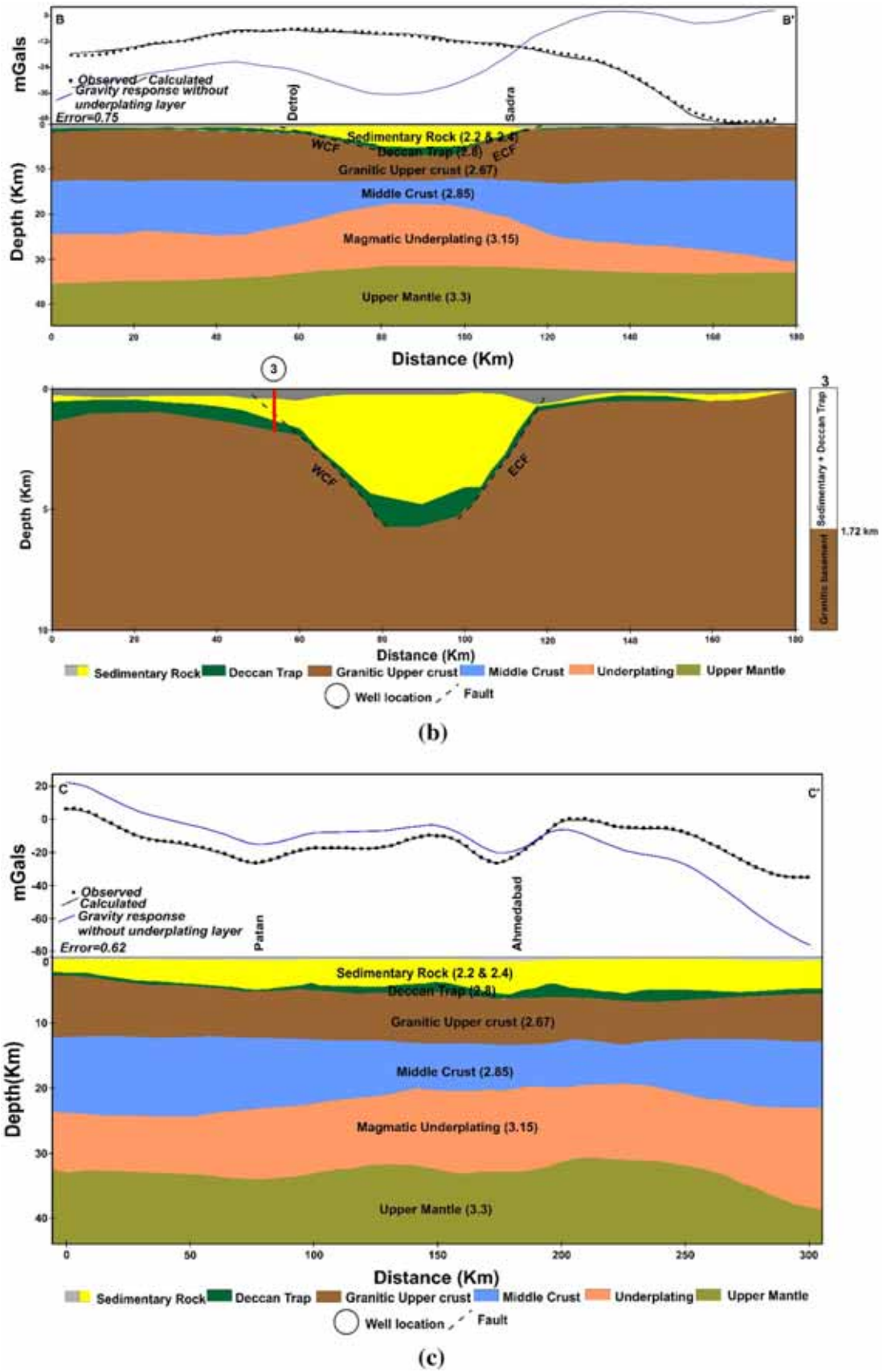


Figure 5. (*Continued.*)

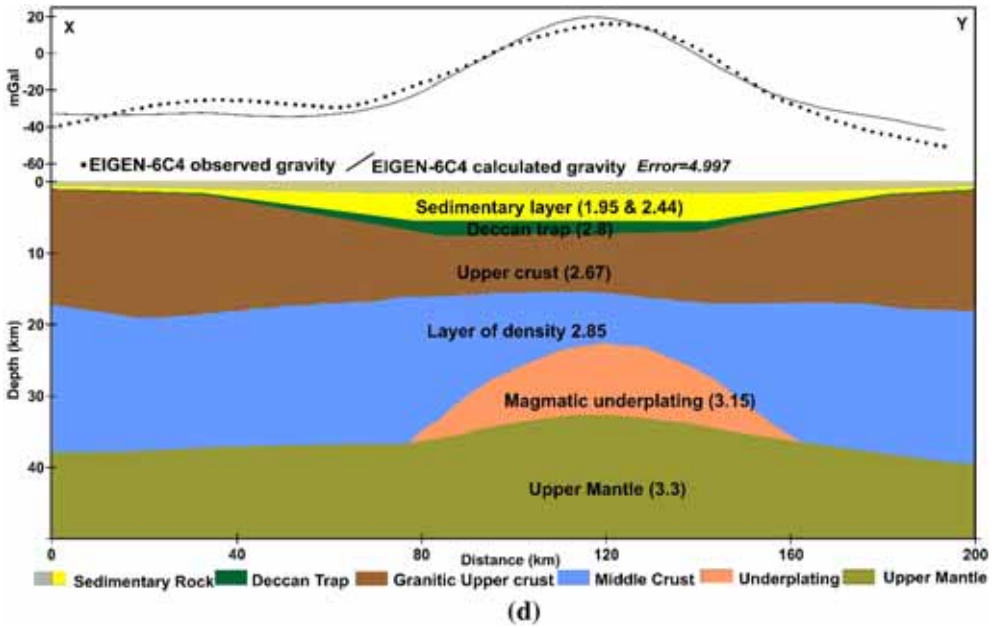


Figure 5. (*Continued.*)

the study area. Calculated Moho depth from the gravity model along the AA′ profile varies between 31 and 33 km (figure 5a).

The density profile BB′ is shown in figure 5(b). This profile passes through drilled well near Detroj, which encountered basement at depth of 1.7 km (Pandey 2012). It is observed that the sedimentary and Deccan Traps thickness are maximum in the central part of the basin while both the layers taper towards the marginal fault, same as in the profile AA′. A high density magmatic underplated layer having the maximum thickness of ∼13 km is also observed in the central part of the basin. The layer merges with Moho in the eastern part while it continues towards the western part. Moho depth variation is found to be 31–34 km along profile BB′. To summarize, it can be said that almost similar crustal structures are observed in both the profiles AA′ and BB′. In both the models AA′ and BB′, thickness of the magmatic underplating is highest at the central part of the basin that decreases towards the eastern Cambay fault, while towards the western Cambay fault, thickness is not decreasing. In view of this, it is inferred that magmatic underplating layer is absent or may have very less thickness in the eastern part of the basin while it is extending in the western part of the basin that is extended up to the Saurashtra peninsula.

The derived density model along a 300 km long profile CC′ (along the basin) is shown in figure 5(c). From the observed gravity values along the section it is found that BA values are higher in the northern part of basin. The model shows that the average sedimentary thickness along the profile is 4–5.5 km and the thickness is highest, ∼5.5 km, in the Gandhinagar area. Variation in thickness of Deccan Traps is between 0.5 and 3 km along the section. Thickness of middle crust along the rift varies between 8 and 12 km. It is also revealed that the magmatic underplated layer is present throughout the profile and its thickness increases in the southern part of the basin, being 15 km. We infer from the present model that the Moho depth variation is 31–34 in the northern part of the basin, while it increases up to 37 km in the southern part of basin.

The BA responses have been computed for all the profiles without the underplated layer for showing the difference in observed and computed gravity responses to vindicate the presence of underplated layer as well as its extension in the CRB. The density of magmatic underplating layer is kept to be the same as of the middle crust, i.e., 2.85 gm/cc. The response of BA without the underplating layer is plotted along with responses calculated using our proposed density model and shown in figure 5. It is clearly observed that if underplating layer is not considered for the

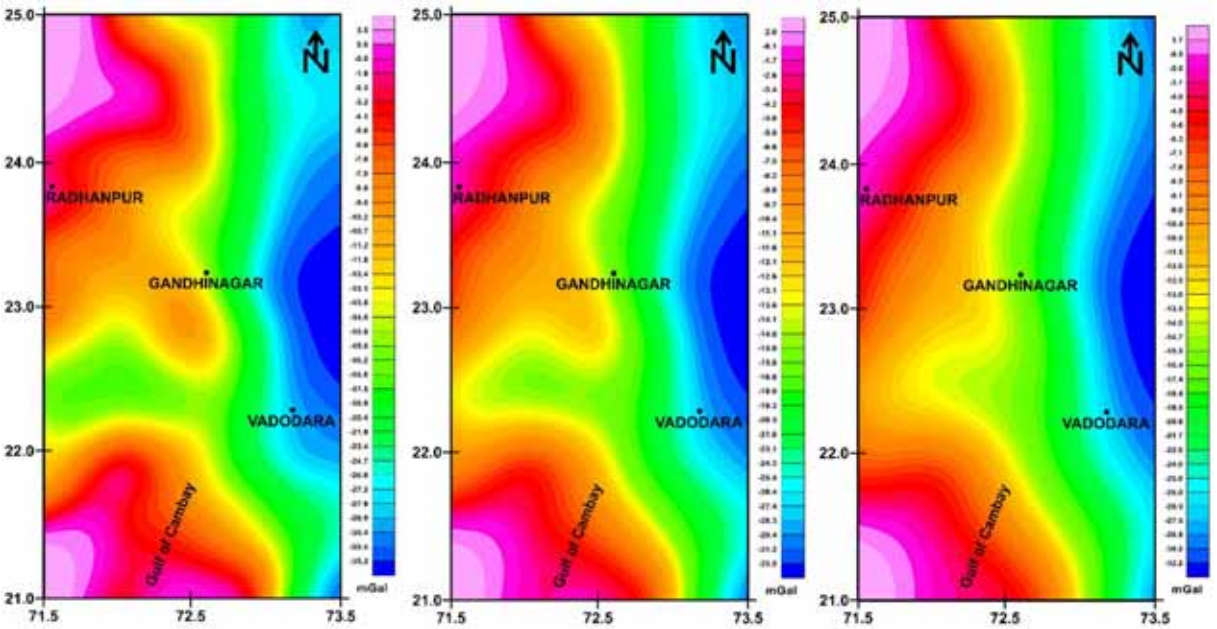


Figure 6. Upward continuation of the Bouguer anomaly at the height of **(a)** 30 km, **(b)** 40 km, and **(c)** 50 km. High value of BA is seen in the western part of the study area, while the eastern part shows comparatively low BA value.

modelling, then large inconsistency is observed between the observed and calculated BA responses. Moreover, the high BA value over H1 in the central part of the CRB can be explained by two possibilities. First, there should be a high density body present in the middle crustal level, like in Saurashtra peninsula and Kachchh rift. The DSS results of Kaila *et al.* (1990) and Dixit *et al.* (2010) do not reveal any high velocity anomaly in the mid crustal level. Therefore, it cannot be accepted to explain the high BA over H1. The second possibility is the presence of high density body in the lower crust that is also confirmed by DSS studies done by Kaila *et al.* (1990), Tewari *et al.* (1991) and Dixit *et al.* (2010). Therefore, high BA value over H1 can only be explained by considering the magmatic underplating layer in the lower crust.

The upward continuation (UC) of the BA value was carried out at different heights of 30, 40 and 50 km (figure 6). Although exact depth estimation is not accurate, the sources of the anomalies for these various maps can be approximated to the depths of 15, 20 and 25 km, respectively. The UC maps of BA values at different heights show high value (1.0–6.5 mGal) in western part of the study area that indicates presence of relatively high density material in the lower crust. The eastern part shows comparatively low BA value (−25 to −34 mGal), which can be correlated with presence of inadequate high density material in the lower crust. This high density material in lower crustal depth is interpreted as magmatic underplating in the present gravity modelling and on the basis of the upward continued BA values, it can be inferred that at deeper depths, the layer is present in the western part while the thickness decreases towards the eastern part of the study area. Similar results are also reported by Tewari *et al.* (1991). They however, opined that the high density layer is only confined in the Cambay basin, which is partially contradicting with the present results. In this context, we would like to mention that the density model of Tewari *et al.* (1991) is only constrained by DSS results of Kaila *et al.* (1990) that gives average depth of the Moho 39–41 and 41–44 km at the eastern and the western Cambay fault, respectively and the magmatic underplating layer in the lower crust is confined only in the Cambay rift (Tewari *et al.* 1991). However, the recent results of the Receiver function and surface wave tomography (SWT) indicate shallow Moho depth (30–35 km) (Chopra *et al.* 2014; Rao *et al.* 2015; Sharma *et al.* 2018). Presence of the magmatic underplating in lower crust is confirmed by DSS studies in the Saurashtra (Rao and Tewari 2005). Teleseismic waveform modelling depicts average crustal P and S wave velocities with higher Poisson's ratio in the Saurashtra region than in the Indian shield, which is mainly associated with the presence of magmatic

underplating in the lower crust (Kumar and Mohan 2014). Recent SWT results also confirm the presence of magmatic underplating layer in the lower crust in Kachchh rift and Saurashtra peninsula (Sharma *et al.* 2018). In view of all these, we can infer that the magmatic underplated layer extends up to the Saurashtra peninsula, which is in contradiction with the density model adapted by Tewari *et al.* (1991). Moreover, short wavelength anomalies are not considered in the density model adapted by Tewari *et al.* (1991). In the present study, we have used the drilled well data as constraint to image the shallow sub-surface features, i.e., short wavelength anomaly. Further, the density model of Tewari *et al.* (1991) along the same profile (XY in figure 2b) has been used to the EIGEN-6C4 data to check the effectiveness of the gravity modelling in the present study. Figure 5(d) represents observed gravity response and the gravity response calculated using the density model of Tewari *et al.* (1991). Because of non-uniqueness in forward gravity modelling, more than one model can be prepared with the same data. It exhibits a small mismatch, though it indicates almost similar anomaly pattern between the observed and modelled gravity responses. Despite, it is inferred that the proposed density model gives more realistic picture of the crust than that of Tewari *et al.* (1991) as used constraints from power spectrum of BA, DSS as well as recent seismological and geophysical studies.

It is observed that magmatic underplated lower crustal layer is thin towards the eastern Cambay fault and merges with the Moho. Because of this fact, the low Bouguer anomaly (L1) is reflected in this part of the study area, even though the basement is shallow. This magmatic underplating layer continues further to the south-west of Saurashtra. We also see that the extent of this magmatic underplated lower crustal layer is not restricted to the study area; it continued up to Narmada–Tapti region in the south, which is also documented by Singh and Meissner (1995). The layer plausibly have its extension in the north also, which needs to be investigated.

Moho depth estimated from the present gravity modelling ranges between 31 and 37 km. In this context, it is mentioned that the Moho depth variation is 36–45 km in the Saurashtra (Radha Krishna *et al.* 2002; Chopra *et al.* 2014; Kumar and Mohan 2014; Rao *et al.* 2015), 38–40 km in the Jambusar–Broach graben (Singh and Meissner 1995), 33–40 km in the Rajasthan (Kilaru *et al.* 2013) and 35–43 km in the Kachchh rift (Chopra *et al.* 2014; Rao *et al.* 2015; Seshu *et al.* 2016). We see that previous studies documented a deeper Moho in the region adjoining the study area. In view of this, it can be argued that the Moho is shallower in the basin than the surroundings. We found that the Deccan trap thickness is maximum in the central part of the Cambay basin, where the underplating layer is found thickest and Moho depth shallowest. Therefore, it is further infered that the gravity high in the central part of the CRB is the combined effect of thick Deccan trap, magmatic underplating and the shallow Moho, although the sedimentary layer is thick in this part. The variation of surface heat flow along the deep seismic sounding (DSS) profile ranges between 82.5 and 84 $mW/m^2$. Gupta (1981) and Thiagarajan *et al.* (2001) argued that the reason for the high heat flow in the Cambay basin is presence of the thin crust and an upwarping mantle. This facilitates an environment for oil and gas formation in organic rich sedimentary rocks of the Cambay basin, similar to the offshore Bombay high (Biswas 1982). Similar deep crustal structure (i.e., uplifted Moho and presence of high density material in the lower crust) is also reported in Kenya rift, Baikal rift, Rio Grande rift and Rhine Graben (Thybo and Artemieva 2013; Thybo and Nielsen 2009).

A comprehensive evolution history of the Cambay rift is illustrated in figure 7. After the break-up of the Indian plate from the Gondwanaland, the western continental margin of the Indian plate traversed in the northward direction, and initiated the rifting of the Kachchh basin in the early Jurassic (Biswas 1982; Dietz and Holden 1970). During this time, West Coast fault and the Narmada geofracture were present (figure 7) (Biswas 1982). Afterwards, the Indian plate rotated anti-clockwise in the Early Cretaceous, and the Cambay rift opened with the extension of West Coast fault along the Dharwar trend (Biswas 1982, 1987). This rifting continued till the Tertiary and is substantiated by the presence of Tertiary sediments in the Cambay basin (Biswas 1982; Tewari *et al.* 1995; Pandey 2012). The existence of the CRB in the Early Cretaceous is confirmed by the presence of Mesozoic sediments below the Deccan traps (Kaila *et al.* 1990; Tewari *et al.* 1995; Dixit *et al.* 2010; Pandey 2012). During the Late Cretaceous, the Indian plate was drifting northward over the Reunion hotspot near the equator (figure 7, Biswas 1982) with a very high speed of 18–20 cm/year (Kumar *et al.* 2007). At the same time ($\sim$65 Ma) the Earth's largest flood basalt, the

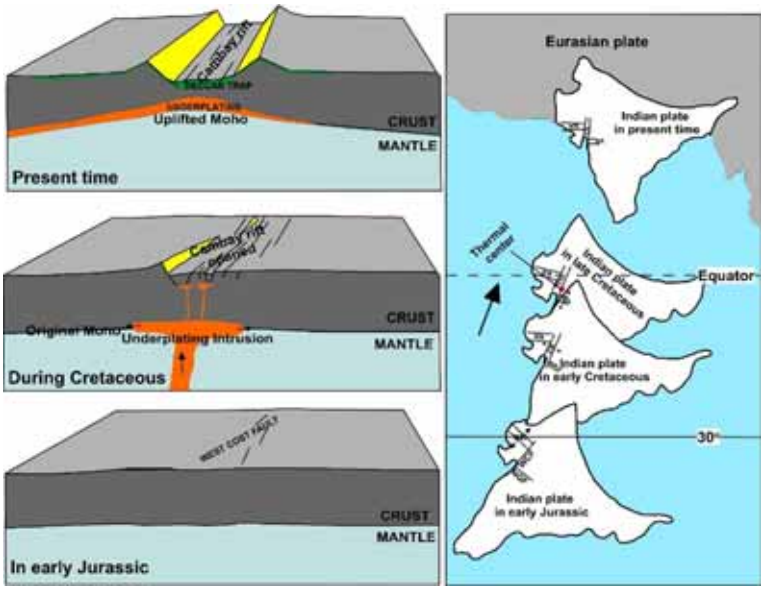


Figure 7. Generalised conceptual model describing the evolution of the Cambay rift basin in different geological time scale with its relation to northward movement of the Indian plate. Location of Indian plate in different geological time is modified after Dietz and Holden (1970) and Biswas (1982). Maps present in this figure are not to the scale.

Deccan trap erupted (Besse and Courtillot 1988; White and McKenzie 1989). During this movement, mantle was thermally eroded and melted partially. Because of the buoyancy force, all the molten material had risen and tried to come up to the surface, but due to lack of buoyant rate most of the material cooled and ponded near the crust-mantle boundary that formed magmatic underplated layer in the lower crust (figure 7, Rao *et al.* 2015). The Deccan trap was formed by the molten material that came out to the surface and was filled in the low lying areas of the rift (Tewari *et al.* 1995; White and McKenzie 1989). This might be the plausible explanation for the large thickness of the Deccan trap in the rift. We infer that since both rifting of the basin and the Deccan volcanism were coeval processes, it resulted together in the magmatic underplating and the crustal thinning of the CRB and is presented in our conceptual model (figure 7). In other words, the Deccan traps, magmatic underplating layer in the lower crust, and crustal thinning over the CRB were developed due to the northward movement of the Indian plate during the Cretaceous.

## 5. Conclusions

The EIGEN-6C4 global gravity model data have been compared with the terrestrial gravity data and found that EIGEN-6C4 data has the sufficient resolution for the study of subsurface structure over the Cambay basin. We note high BA values ranging from +20 to −50 mGal within the basin, which are almost in accordance with results of earlier studies in this area. The results of the present gravity modelling along the three profiles reveal presence of large sedimentary thickness along the central part of the CRB. This thickness decreases towards both the marginal faults of the basin. The sedimentary rock is deposited on the floor of the Deccan Traps, which has higher thickness in the central part of the basin and tapers towards both the marginal faults. A thin layer of Deccan Traps of thickness ∼1.5–3 km, and the magmatic underplating layer of thickness ∼7–15 km are seen throughout the basin.

A detailed insight into the crustal structure of Cambay rift basin is presented, which play an important role for the study of geodynamics in this area. We conclude that shallow Moho depth together with presence of magmatic underplated layer in the lower crust are possibly the reason for the higher BA value within the basin. Gravity model and upward continuation show the magmatic underplating layer is either absent or has very less thickness in eastern part of ECF, and this may be the plausible reason for low gravity. The magmatic underplating layer in lower crust and crustal thinning over the CRB are the result of the northward movement of the Indian plate during the Cretaceous. All together the crustal thickness estimated in the present study is in accordance

with those obtained by previous shallow subsurface studies. However, our results provide a better understating of the shallow subsurface geology. The outcome of this study would help the petroleum geologists and geophysicists immensely towards hydrocarbon exploration in this region.

## Acknowledgements

We thank the Editor and Reviewer for the constructive comments that greatly improved the manuscript. Authors are thankful to Dr M Ravi Kumar, Director General, ISR for his suggestions that have resulted in significant improvement in the manuscript. AKC thanks Dr A P Singh, Chief Scientist, CSIR–NGRI for his help regarding the gravity modelling. The authors also thank Prof Saibal Gupta, IIT Kharagpur, for his constructive suggestions during preparation of the manuscript. International Centre for Global Earth Models (ICGEM) is gratefully acknowledged for making the EIGEN-6C4 gravity data available to the users.

## References

Andersen O B, Knudsen P and Berry P A M 2010 The DNSC08GRA global marine gravity field from double retracked satellite altimetry; *J. Geodesy* **84** 191–199.

Avasthi D N, Ramakotaiah G, Varadarajan S, Rao N D J and Behl G N 1971 Study of the Deccan Traps of Cambay Basin by geophysical methods; *B. Volcanologique* **35** 743–749.

Barton P J 1986 The relationship between seismic velocity and density in the continental crust – a useful constraint? *Geophys. J. Roy. Astr. S.* **87** 195–208.

Besse J and Courtillot V 1988 Paleogeographic maps of the continents bordering the Indian ocean since the Early Jurassic; *J. Geophys. Res.* **93** 11,791–11,808.

Bhattacharji S, Sharma R and Chatterjee N 2004 Two- and three-dimensional gravity modeling along western continental margin and intraplate Narmada-Tapti rifts: Its relevance to Deccan flood basalt volcanism; *Proc. Indian Acad. Sci. (Earth Planet. Sci.)* **113** 771–784.

Biswas S K 1982 Rift basins in western margin of India and their hydrocarbon prospects with special reference to Kutch Basin; *AAPG Bull.* **66** 1497–1513.

Biswas S K 1987 Regional tectonic framework, structure and evolution of the western marginal basins of India; *Tectonophys.* **135** 307–327.

Blakely R J 1995 *Potential Theory in Gravity and Magnetic Applications*; Cambridge University Press, pp. 182–210, 311–358.

Bomfim E P, Braitenberg C and Molina E C 2013 Mutual evaluation of global gravity models (EGM2008 and GOCE) and terrestrial data in Amazon Basin, Brazil; *Geophys. J. Int.* **195(2)** 870–882.

Brocher T M 2005 Empirical relations between elastic wavespeeds and density in the Earth's crust; *Bull. Seismol. Soc. Am.* **95** 2081–2092.

Chandra U 1977 Earthquakes of peninsular India – a seismotectonic study; *Bull. Seismol. Soc. Am.* **67** 1387–1413.

Chopra S, Chang T M, Saikia S, Yadav R B S, Choudhury P and Roy K S 2014 Crustal structure of the Gujarat region, India: New constraints from the analysis of teleseismic receiver functions; *J. Asian Earth Sci.* **96** 237–254.

Christensen N I and Mooney W D 1995 Seismic velocity structure and composition of the continental crust: A global view; *J. Geophys. Res.* **100** 9761–9788.

Dhar P C and Bhattacharya S K 1993 Status of Exploration in the Cambay Basin; In: *Proceedings second seminar on petroliferous basins of India,* Indian Petroleum Publishers, Dehradun, **2(79)** 1–32.

Dietz R S and Holden J C 1970 Reconstruction of Pangaea, breakup and dispersion of continents, Permian to present; *J. Geophys. Res.* **75** 4939–4956.

Dixit M M, Tewari H C and Rao C V 2010 Two-dimensional velocity model of the crust beneath the South Cambay Basin, India from refraction and wide-angle reflection data; *Geophys. J. Int.* **181** 635–652.

Director General of Hydrocarbon (DGH), Government of India (GOI) website, 2017: http://dghindia.gov.in//assets/downloads/56cfe9a4c0c6eThe_Cambay_rift_Basin.pdf.

Dobrin M B and Savit C H 1988 *Introduction to Geophysical Prospecting*; 4th edn, McGraw-Hill International Editions, pp. 581–632.

Forsberg R and Skourup H 2005 Arctic Ocean gravity, geoid and sea-ice freeboard heights from ICESat and GRACE; *Geophys. Res. Lett.* **32** 1–4.

Förste C, Bruinsma S L, Abrikosov O, Lemoine J M, Marty J C, Flechtner F, Balmino G, Barthelmes F and Biancale R 2014 EIGEN-6C4 The latest combined global gravity field model including GOCE data up to degree and order 2190 of GFZ Potsdam and GRGS Toulouse. GFZ Data Services.

Gupta H K, Mohan I and Narain H 1972 The Broach earthquake of March 23, 1970; *Bull. Seismol. Soc. Am.* **62** 47–61.

Gupta M L 1981 Surface heat flow and igneous intrusion in the Cambay Basin, India; *J. Volcanol. Geotherm. Res.* **10** 279–292.

Jacobsen B H 1987 A case for upward continuation as a standard separation filter for potential-field maps; *Geophysics* **52** 1138–1148, https://doi.org/10.1190/1.1442378.

Kaila K L, Tewari H C, Krishna V G, Dixit M M, Sarkar D and Reddy M S 1990 Deep seismic sounding studies in the north Cambay and Sanchor basins, India; *Geophys. J. Int.* **103** 621–637.

Kailasam L N and Quereshy M N 1964 On some anomalous Bouguer gravity anomalies in Indian in advancing frontier in Geology and Geophysics; *Indian Geophys. U.*, pp. 135–146.

Kilaru S, Goud B K and Rao V K 2013 Crustal structure of the western Indian shield: Model based on regional gravity and magnetic data; *Geosci. Frontiers* **4** 717–728.

Krishnamurthy P, Gopalan K and Macdougall J D 2000 Olivine composition in picrate basalt and the Deccan volcanic cycle; *J. Petrol.* **41** 1057–1069.

Kumar P and Mohan G 2014 Crustal velocity structure beneath Saurashtra, NW India, through waveform

modeling: Implications for magmatic underplating; *J. Asian Earth Sci.* **79** 173–181.

Kumar P, Yuan X, Kumar M R, Kind R, Li X and Chadha R K 2007 The rapid drift of the Indian tectonic plate; *Nature* **449** 894–897.

Kundu J, Wani M R and Thakur R K 1993 Structural style in South Cambay rift and its control on post-rift deltaic sedimentation; Proceedings second seminar on Petroliferous Basins of India, Indian Petroleum Publishers, Dehradun, **2** 79–96.

Lowrie W 2007 Gravity, the figure of the Earth and geodynamics; In: *Fundamentals of Geophysics,* 2nd edn, Cambridge: Cambridge University Press.

Ludwig J W, Nafe J E and Drake C L 1970 Seismic refraction; In: *The Sea* (ed.) Maxwell A E, Wiley Inter Science, New York **4** 53–84.

Maus S and Dimri V 1996 Depth estimation from the scaling power spectrum of potential fields? *Geophys. J. Int.* **124** 113–120.

Merh S S 1995 Geology of Gujarat, India; Geological Society of India, 222p.

Mishra M and Patel B K 2011 Gas shale potential of Cambay formation, Cambay basin, India; Proceedings: The 2nd South Asian Geoscience Conference and Exhibition, GEOIndia-2011, pp. 1–5.

Mishra D C 2011 *Gravity and Magnetic methods for Geological studies: Principles, Integrated Exploration and Plate Tectonics;* BS Publications, 958p.

Mohan K, Kumar G P, Chaudhary P, Choudhary V K, Nagar M, Khuswaha D, Patel P, Gandhi D and Rastogi B K 2017 Magnetotelluric investigations to identify geothermal source zone near Chabsar hotwater spring site, Ahmedabad, Gujarat, Northwest India; *Geothermics* **65** 198–209.

Nabhakumar K, Lakra M N, Kumar D and Niyogi K 2012 Estimation of thickness of Deccan trap in Broach Jambusar block of Cambay basin – an innovative approach; 9th Biennial international conference and exposition on petroleum geophysics, Hyderabad, 114p.

Narayan S, Sahoo S D, Pal S K, Kumar U, Pathak V K, Majumdar T J and Chouhan A 2017 Delineation of structural features over a part of the Bay of Bengal using total and balanced horizontal derivative techniques; *Geocarto Int.* **32** 351–366.

Oasis Montaj MAGMAP manual: http://updates.geosoft.com/downloads/files/how-to-guides/Getting_Started_with_montaj_MAGMAP_Filtering.pdf.

Oasis Montaj GMSYS manual: http://updates.geosoft.com/downloads/files/how-to-guides/GM-SYS_Profile_Create_New_Model.pdf.

Pandey U S D 2012 Petroleum exploration in Mesozoic basins in Western onshore India; 9th Biennial International Conference & Exposition on petroleum geophysics, Hyderabad.

Pal S K, Narayan S, Majumdar T J and Kumar U 2016 Structural mapping over the 85°E Ridge and surroundings using EIGEN6C4 high-resolution global combined gravity field model: An integrated approach; *Mar. Geophys. Res.* **37** 159–184.

Pal S K and Majumdar T J 2015 Geological appraisal over the Singhbhum–Orissa Craton, India using GOCE, EIGEN-6C2 and in situ gravity data; *Int. J. Appl. Earth Obs.* **35** 96–119.

Pavlis N K, Holmes S A, Kenyon S C and Factor J K 2013 Erratum: Correction to the development and evaluation of the earth gravitational model 2008 (EGM2008); *J. Geophys. Res.: Solid Earth.*

Radha Krishna M, Verma R K and Purushotham A K 2002 Lithospheric structure below the eastern Arabian Sea and adjoining West Coast of India based on integrated analysis of gravity and seismic data; *Mar. Geophys. Res.* **23** 25–42.

Rao B S R and Murthy I V R 1978 *Gravity and magnetic methods of prospecting*; Arnold-Heinemann Publishers, New Delhi, 390p.

Rao G S P and Tewari H C 2005 The seismic structure of the Saurashtra crust in northwest India and its relationship with the Réunion Plume; *Geophys. J. Int.* **160** 318–330.

Rao K M, Kumar M R and Rastogi B K 2015 Crust beneath the northwestern Deccan Volcanic Province, India: Evidence for uplift and magmatic underplating; *J. Geophys. Res.: Solid Earth* **120** 3385–3405.

Seshu D, Rama Rao P and Naganjaneyulu K 2016 Three-dimensional gravity modelling of Kutch region, India; *J. Asian Earth Sci.* **115** 16–28.

Sharma J, Kumar M R, Roy K S and Roy P N S 2018 Seismic Imprints of Plume-Lithosphere Interaction beneath the Northwestern Deccan Volcanic Province; *J. Geophys. Res.: Solid Earth* **123** 10,831–10,853.

Singh A P and Meissner R 1995 Crustal configuration of the Narmada–Tapti region (India) from gravity studies; *J. Geodyn.* **20** 111–127.

Spector A and Grant F S 1970 Statistical models for interpreting aeromagnetic data; *Geophysics* **35** 293–302.

Studinger M and Miller H 1999 Crustal structure of the Filchner-Ronne shelf and Coats Land, Antarctica, from gravity and magnetic data: Implications for the breakup of Gondwana; *J. Geophys. Res.* **104(B9)** 20,379–20,394.

Talwani M, Worzel J L and Landisman M 1959 Rapid gravity computations for two-dimensional bodies with application to the Mendocino submarine fracture zone; *J. Geophys. Res.* **64** 49–59.

Tapley B D, Bettadpur S, Ries J C, Thompson P F and Watkins M M 2004 GRACE measurements of mass variability in the Earth system; *Science* **305** 503–505.

Tewari H C, Dixit M M, Sarkar D and Kaila K L 1991 A crustal density model across the Cambay basin, India, and its relationship with the Aravallis; *Tectonophys.* **194** 123–130.

Tewari H C, Dixit M M and Sarkar D 1995 Relationship of the Cambay rift basin to the Deccan volcanism; *J. Geodyn.* **20** 85–95.

Tewari H C, Rao G S P and Prasad B R 2009 Uplifted crust in parts of western India; *J. Geol. Soc. India* **73** 479–488.

Thiagarajan S, Ramana D V and Rai S N 2001 Seismically constrained two-dimensional crustal thermal structure of the Cambay basin; *Proc. Indian Acad. Sci.* (*Earth Planet. Sci.*) **110** 1–8.

Thybo H and Artemieva I M 2013 Moho and magmatic underplating in continental lithosphere; *Tectonophys.* **609** 605–619.

Thybo H and Nielsen C A 2009 Magma-compensated crustal thinning in continental rift zones; *Nature* **457** 873–876.

Vaish J and Pal S K 2015 Geological mapping of Jharia Coalfield, India using GRACE EGM2008 gravity data: A vertical derivative approach; *Geocarto. Int.* **30** 388–401.

White R S and McKenzie D P 1989 Magmatism at rift zones: The generation of volcanic continental margins and flood basalts; *J. Geophys. Res.* **94** 7685–7729.

Withjack M O, Schlische R W and Olsen P E 2002 Rift-basin structure and its influence on sedimentary systems; In: *Sedimentation in Continental Rifts* (SEPM (Society for Sedimentary Geology)), pp. 57–81.

Zeng H, Xu D and Tan H 2007 A model study for estimating optimum upward-continuation height for gravity separation with application to a Bouguer gravity anomaly over a mineral deposit, Jilin province, northeast China; *Geophysics* **72(4)** 145–150.

Corresponding editor: N V Chalapathi Rao